University of
HUDDERSFIELD

University of Huddersfield Repository

Albarbar, A., Gu, Fengshou and Ball, Andrew

Diesel engine fuel injection monitoring using acoustic measurements and independent component analysis

Original Citation

Albarbar, A., Gu, Fengshou and Ball, Andrew (2010) Diesel engine fuel injection monitoring using acoustic measurements and independent component analysis. Measurement, 43 (10). pp. 1376-1386. ISSN 0263-2241

This version is available at http://eprints.hud.ac.uk/8384/

Accepted Manuscript
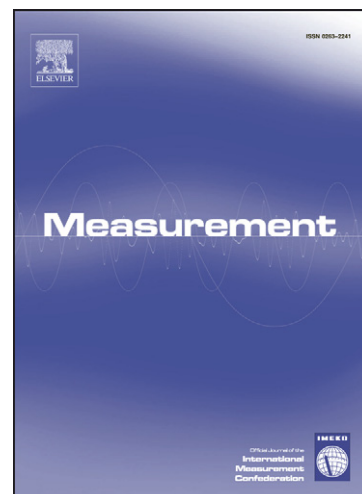
Diesel engine fuel injection monitoring using acoustic measurements and independent component analysis

A. Albarbar, F. Gub, A.D. Ball

Diesel engine fuel injection monitoring using acoustic measurements and independent component analysis

A. Albarbar[1]*, F. Gu[2], A. D. Ball[2]

[1]*Department of Engineering and Technology,
Manchester Metropolitan University, Manchester, M1 5GD*
[2]*Computing and Engineering, University of Huddersfield
Queensgate, Huddersfield, HD1 3DH*

ABSTRACT

Air-borne acoustic based condition monitoring is a promising technique because of its intrusive nature and the rich information contained within the acoustic signals including all sources. However, the back ground noise contamination, interferences and the number of Internal Combustion Engine ICE vibro-acoustic sources preclude the extraction of condition information using this technique. Therefore, lower energy events; such as fuel injection, are buried within higher energy events and/or corrupted by background noise.

This work firstly investigates diesel engine air-borne acoustic signals characteristics and the benefits of joint time-frequency domain analysis. Secondly, the air-borne acoustic signals in the vicinity of injector head were recorded using three microphones around the fuel injector (120° apart from each other) and an Independent Component Analysis (ICA) based scheme was developed to decompose these acoustic signals. The fuel injection process characteristics were thus revealed in the time-frequency domain using Wigner-Ville distribution (WVD) technique. Consequently the energy levels around the injection process period between 11 and 5 degrees before the top dead center and of frequency band 9 to 15 kHz are calculated. The developed technique was validated by simulated signals and empirical measurements at different injection pressure levels from 250 to 210 bars in steps of 10 bars. The recovered energy levels in the tested conditions were found to be affected by the injector pressure settings.

KEYWORDS

Condition Monitoring, Internal Combustion Engine (ICE), Fuel Injector, Air-borne Acoustics, Blind Source Separation (BSS), Independent Component Analysis (ICA), Wigner-Ville Distribution (WVD).

1. INTRODUCTION

The increasing interest in environmental problems has necessitated the improvement of engine performance, and reduction of noise and pollutant emissions. One of the key components, which determine engine torque, emissions, noise quality and fuel consumption, are the fuel injection equipment and the intake management system. The effects of the injection timing on the engine emissions and exhaust gas have been studied in [1]. Injection pressure, fuel quantity, injector opening and closing timings are the keys to the ideal injection process condition monitoring system. These parameters should be kept at their optimum values to reduce the fuel consumption and pollutant emissions, and increase the output power. However, measuring these parameters could not be done without fixing sensors and introducing a permanent damage into the system which may influence these parameters e.g. needle lift and injection pressure measurement. Injection process induced noise and air-borne acoustic signals have been sporadically studied for many years. However, previous work has focused on topics other than the noise radiated from the injector itself [2, 3, 4]. The moving

mass inside the injector is a small in the order of 15 grams, and this mass takes a very short time, in the order of 1-3 milliseconds, from the fully open to fully closed position. There is a distinct opening and closing vibrations and acoustic signals for most injectors. The opening vibrations and induced acoustic signals are due to the moving mass hitting the upper stop and the closing ones are due to the moving mass hitting the seat. As a result, the acoustic signals induced by the diesel injector are very short click, with broad frequency content, and radiated from the surface of the injector itself or transmitted through the fuel system or the engine block. Unfortunately, these diagnostic signatures are dominated by the other energy sources and corrupted by background and interference noises.

Most of the work in the literature on diesel fuel injection has been devoted to describing the noise and vibration generated by the fuel pumps and fuel lines. Injector dynamics, needle movements and their resulting vibrations were studied by Gu and Ball [5, 6]. They described the vibration characteristics of injectors by three series of transients during an injection cycle; fluid excitation commencing prior to needle impact, needle opening impact and needle closing impact. The injection process was also studied by Gill et al [7] using acoustic emission and has achieved better results than vibration signatures in detecting the pressure build up activities prior the opening of the needle valve. The injection and exhaust valves opening and closing events were also studied using acoustic emissions in [8]. In this work the injection induced air-borne acoustic signals measurements were recorded remotely and ICA based scheme was developed to monitor injector operation parameters. Figure 1(a) shows engine (4 cylinders, direct injection) airborne acoustic signals measured using a microphone located 1m above the floor and 1m away from the cylinder manifold with the engine running at an average speed of 1000rpm (16.7Hz) and with no load [9, 10, 11].

Figure 1 Airborne acoustic signal representations at zero load and 1000 rpm, microphone 1m from the engine and 1 m above laboratory floor (a) time domain (b) frequency domain (c) time-frequency contour plots

The airborne acoustic signal shown in Figure 1(a) was enhanced by averaging. In practice, it is frequently the case that with a repeated signal, the signal to noise ratio can be improved by averaging, particularly where the corruption of the signal is due to unwanted noise occurring as a result of

random events. Time-domain averaging is a way to reduce the content of undesired components in a signal.

The main feature could be observed from the acoustic waveform, shown in Figure 1(a), is four peaks corresponding to the engine firing sequence and these represent combustion events in the cylinders 3, 1, 2 and 4 respectively. What makes the waveform complicated and difficult to extract information from is the numerous frequency components superimposed on each other. In the associated power spectrum, shown in Figure 1(b), four peaks can be seen; the first at twice the frequency of revolution (33.4 Hz), the second at four times the frequency of revolution (66.8 Hz), the third at 100 Hz and the fourth at 470 Hz. The amplitudes of any higher harmonics can be ignored because they contain considerably less energy than the first four leading terms. Each cylinder experiences fuel injection and combustion once for every two complete revolutions of the crankshaft. Thus the number of 'combustions' per single revolution of the camshaft will be equal to (number of cylinders)/2. Here there are four cylinders, so there will be two combustion processes during each complete revolution of the camshaft, and the corresponding noise peak will occur at twice the fundamental frequency (2 x 16.7 ≈ 33 Hz). The amplitude of this peak is highly dependent on the combustion conditions. The second peak (67 Hz) is probably due to closing knock of the valves, which occur twice per crankshaft revolution, every second revolution in each cylinder. By increasing the load the amplitude of both of these peaks increase. The third peak at 100 Hz, which corresponds to the third harmonic of the firing frequency, also increases in amplitude at higher loads. It has been shown that the peaks at 100 and 470 Hz are due to the vibration of the oil sump and front timing gear cover [12].

Figure 1(c) shows the acoustic waveform of the diesel engine in the time frequency domain using the Wigner-Ville distribution (WVD). From the WVD representation we can see clearly four peaks representing the combustion events of the engine cylinders in the firing order from left to right (3, 1, 2, and 4). The spectral analysis shows that the major part of the energy is located in the lower frequencies (below 5 kHz), this can be seen more clearly in the WVD representation, and also we can see that the peak of the WVD extends to around 35 kHz.

Clearly, no weak events could be observed from Figure 1; although we know the exact time of some of these events, the occurrence of the event around cylinder#1 is shown in Figure 2. The features of such weak events are dominated by other higher energy sources and/or buried in a high-level of background noise, so it is necessary to extract them from such background noise to accurately evaluate the injection process condition. Traditional methods seem incapable of solving such problems because the background noise contains not only Gaussian noise but also disturbances from other sources and the adjacent machines; coherent filtering techniques and adaptive noise cancelling (ANC) could be used to improve the signal to noise ratio of a diagnostic signal. The drawback of these two methods is that the first relies on a synchronizing signal and the second needs a reference signal which is not available in this case [13, 14]. BSS and ICA provide a new technique for solving these problems making its application to machine fault diagnosis very attractive.
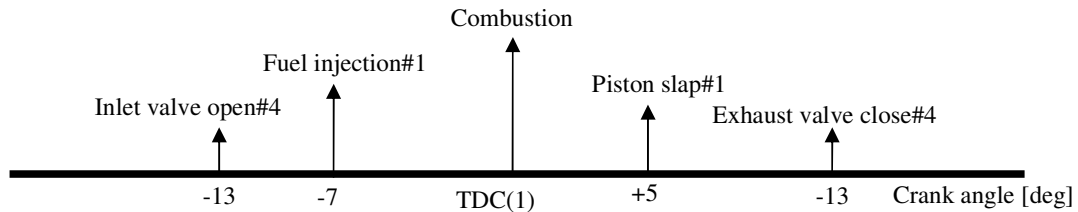

Figure 2 Theoretical occurrences of engine noise sources around cylinder#1

The application of Independent Component Analysis (ICA) in machine fault diagnosis has been developing rapidly and provides a new technique for the separation of source signals under high-level

3

background noise and, thus, the possibility of enhancing these weak and corrupted features. It should be possible for ICA to be used for: noise cancellation, the extraction of weak signals, the separation of sources, feature extraction and pattern classification.

Gelle et al [15] have applied the BSS technique to machine fault diagnosis, using BSS as a pre-processing step for the detection and diagnosis of faults in rotating machinery. Gelle's paper compares temporal and frequency based approaches to the solution of the BSS problem for rotating machine signals. Roam [16] proposed an adaptive BSS algorithm based on information maximisation, and applied this technique to gear tooth failure detection and analysis. Because a signal to noise ratio improvement alone does not sufficiently enhance a machine signal to allow fault evaluation, Knaak [16] proposed an assessment for BSS algorithms to verify their applicability with respect to machine signals.

Ypma in [18] suggested a novel approach to fault detection in rotating machinery. He proposed that ICA was used to combine various vibration measurements made on a machine to produce a vector domain description which would be compared with an admissible domain indicating normal machine operation. This approach was successfully applied to the monitoring and diagnosis of a submersible pump.

Tian et al. [19] combined ICA in the frequency domain (ICA-FD) with Morlet wavelet filtering for gearbox fault diagnosis. Vibration signals from a gearbox were separated into two components using ICA-FD. Morlet wavelet filtering was then applied to the separated components. Better diagnosis was obtained with this combination compared to using wavelet filtering alone. ICA techniques were applied to a diesel engine by Li et al. [20] in an attempt to identify diesel engine noise sources.

In the work reported here, an air-borne acoustic signals and ICA algorithm based scheme was developed to extract some of these hidden features and consequently utilise these features for monitoring the injector health. Firstly the dominant harmonics were removed, secondly a proposed ICA algorithm was applied to decompose the residual signal, thirdly the injector operation induced acoustic signals were estimated in the time-frequency domain using the Wigner-Ville distribution (WVD) and finally the energy levels around the injection process event between 11 and 5 degrees before the top dead centre (TDC) were calculated and were found to be directly affected by the injector condition.

It is evident that the proposed procedure has given clearer results to monitor the injector opening and closing induced air-borne acoustic signals. More importantly, signal to noise ratio improvement allows various statistical methods to be successfully used in diagnosing other and compound faults.

Section 2 in this paper introduces the ICA algorithm structure; the application of this algorithm on a modelled engine induced air-borne acoustic signals are also presented. The instrumentation test rig facilities and the exploitation of ICA algorithm on a working engine measured air-borne acoustics are described in section 3. Fault simulation and the experimental results are presented in section 4. In section 5 a summary is given and few conclusions are outlined.

2. THEORY AND BACKGROUND

BSS is a technique for separating the independent components of mixed signals recorded by different sensors when the source of the signals and transmission channels are unknown. BSS comprises independent component analysis (ICA) [21]. Here "blind" have two meanings [22]:

1- The system inputs cannot be directly observed,

2- The mixture form (mixing matrix) of sources is unknown.

Obviously, the mathematical model for the relationship between the sources and the sensors is not well defined, and the BSS may be described as in Equation 1.

4

$$x(t) = A * s(t) + n(t) \qquad (1)$$

where $x(t) = [x_1(t), x_2(t), \dots, x_m(t)]^T$ is an m-dimensional vector representing the observations, $s(t) = [s_1(t), s_2(t), \dots, s_n(t)]^T$ is an n-dimensional vector representing the sources which are unknown, but mutually statistically independent, A is an unknown mixing matrix, and $n(t) = [n_1(t), n_2(t), \dots, n_m(t)]^T$ is an m-dimensional vector representing the background or extraneous noise and will have the same number of dimensions as the observation vector. The number of sources is assumed to be smaller than or equal to the number of measurements $(n \leq m)$. The operation symbol "*" denotes the 'product' in the instantaneous mixture, and the 'convolution' in the convolutive mixture.

Figure 3 shows a fairly general BSS model and the process often referred to as blind signal decomposition or blind source extraction.

It is clear that in order to perform separation, the demixing matrix, W should approximate A^{-1} and many approaches have been applied to solve this problem. ICA methods estimate the demixing matrix W by exploiting the non-Gaussian nature of signals and the statistical independence of the separated signals. Figure 4 illustrates the general process of BSS.

Without any prior knowledge of the sources or the manner in which their signals combine - the mixing matrix - BSS has two inherent indeterminacies: - the order and magnitude of the sources. However, because of the information the sources preserve in their waveforms these indeterminacies do not affect the correctness of the signal separation.

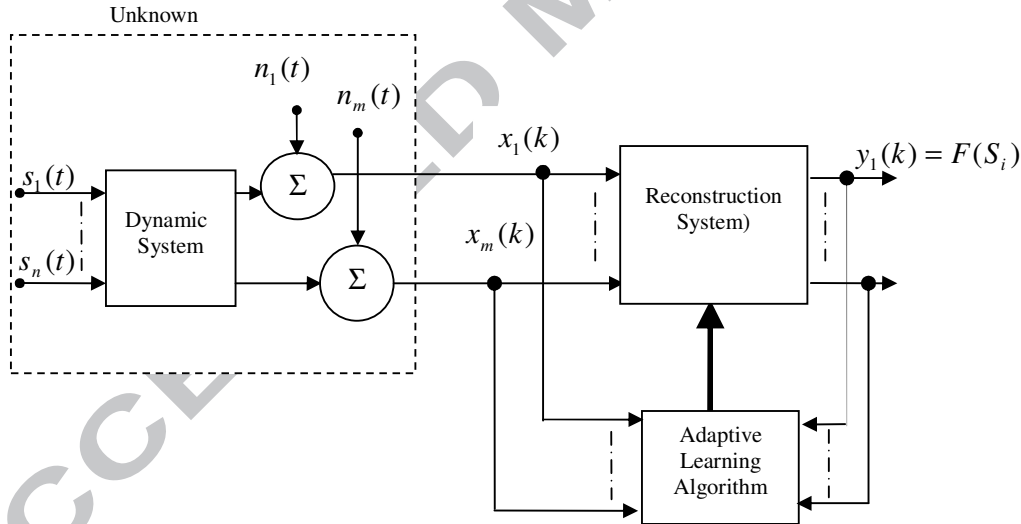Figure 3 General model illustrating blind source separation.

General BSS solution consists of two parts: an objective function and an optimisation algorithm. The estimation of sources is obtained by optimising an objective function. The objective function is the most important element for BSS, and for different objective functions, there are different approaches to BSS and one of them is explained next.

5

$$\begin{bmatrix} s_1(t) \\ s_2(t) \\ .... \\ s_n(t) \end{bmatrix} \Rightarrow \boxed{A(t)} \xrightarrow{x(t)} \Sigma \Rightarrow \boxed{W} \Rightarrow \begin{bmatrix} r_1(t) \\ r_2(t) \\ .... \\ r_m(t) \end{bmatrix}$$

Unknown primary sources · Unknown mixing matrix · Observable mixed signals · Estimated demixing matrix · Separated output signals · $n(t)$
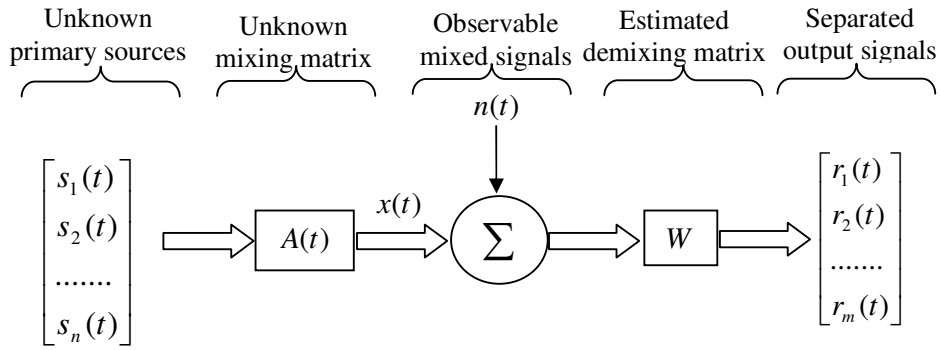
Figure 4 Blind source separation frame work

The developed monitoring scheme is based upon an ICA algorithm; this algorithm was introduced for the first time in 1997 [20]. This algorithm calculates projections that maximize non-Gaussianity measured by an objective function J. Kurtosis $E(y^4) - 3(E(y^2))^2$ (applies to a zero mean variable y) was originally used as a basis for this objective function.

Such a function is sensitive to outliers, and to overcome this it has been proposed to use alternative, more robust objective functions, where the data is first whitened [23, 24]. It was suggested that this could be done using Principal Component Analysis (PCA). PCA is a classical statistical method for obtaining an orthogonal transformation, E, for dimension reduction which maximises the remaining data variance. Figure 5 describes this procedure. A necessary condition that two variables are independent is that they are uncorrelated, and one way of making the basic ICA problem easier is to whiten the original signals, X. Thereafter, it suffices to rotate the whitened data Z suitably, i.e., to find an orthogonal demixing matrix that produces estimates for the independent components S = W*Z. When the whitening is performed by the demixing matrix for the original, centered data is $W = W * \Lambda^{\frac{-1}{2}} E^T$.
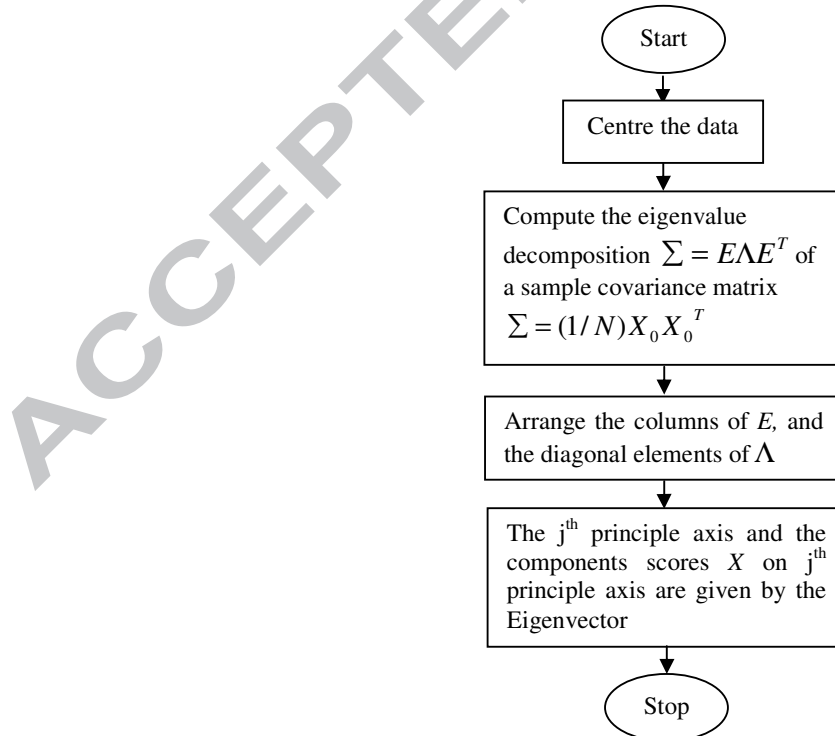

Figure 5 Computing principle components of a data set X

6

A symmetrical version of the ICA algorithm, where all independent components are estimated simultaneously, is described graphically in Figure 6. The algorithm works as follows:

1. Whiten the data. For simplicity, the whitened data vectors are denoted by x and the mixing matrix for whitened data by W.

2. Initialize the demixing matrix $W = [w_1^T \quad w_2^T \quad w_M^T]$, e.g., randomly.

3. Compute new basis vectors using the update rule

$$w_j : \quad = E(g(w_j^T x)x) - E(g'(w_j^T x))w_j \qquad (2)$$

where g is a non-linearity derived from the objective function J, in the case of kurtosis it becomes $g(u) = u^3$, and in case of skewness $g(u) = u^2 g$. Use sample estimates for expectations.

4. Orthogonalize the new W, e.g., by $W = W(W^T W)^{\frac{-1}{2}}$

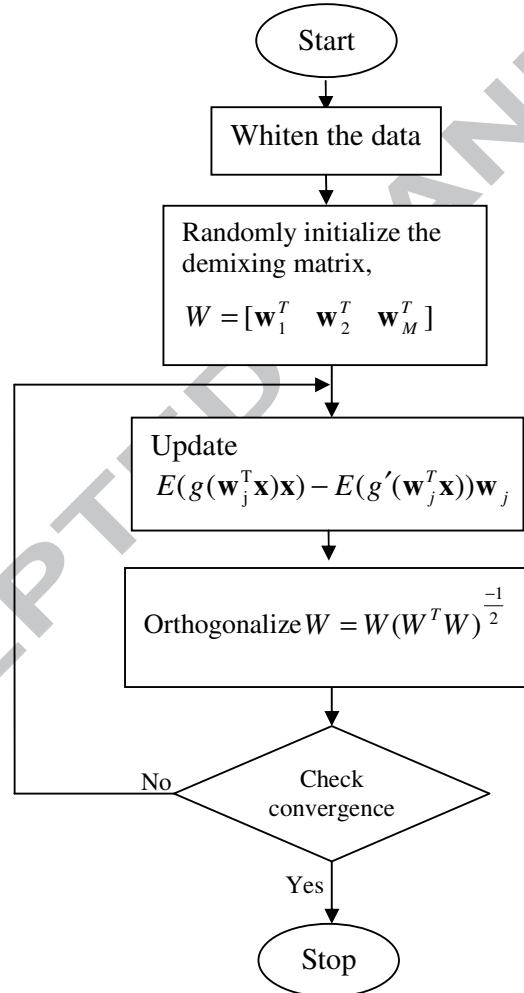5. Repeat from step 3 until convergence.

Figure 6 Implementation of the proposed Fast ICA algorithm

7

The Fast ICA is an appealing algorithm for both practical and theoretical reasons [25]. It has very competitive computational and convergence properties and the Fast ICA is not restricted to resolving either super- or sub-Gaussian sources of the original sources as occurs with many algorithms [22,23][1].

3. AIR-BORNE ACOUSTICS MODELLING

Here, we will illustrate with an example the application of the proposed ICA algorithm to the separation of modelled diesel engine air-borne acoustic signals. The air-borne acoustic signals from ICE e.g. diesel engine are composed of many components emitted from different sources. These sources include combustion, mechanical, and a combination of both. Understanding the components of the air-borne acoustic signal is essential to identify the requirements for acoustic signal analysis. Table 1 briefly summarises diesel engine air-borne acoustic signals excitation forces, their generation mechanisms and transmission paths.

Combustion noise is produced by the rapid rate of increase of cylinder pressure, which besides being a source of engine structural vibrations also excites resonances in the gas inside the combustion chamber cavity. The latter is also a source of vibration and air-borne acoustics.

Table1 Excitation forces and their generation mechanism in diesel engines

Excitation Source	Force applied to structure	Vibration Transmission	Noise Emitter
Combustion Excitation	Rapid rate of change in cylinder pressure (pulses)	Cylinder head, Piston and connecting mechanisms	Manifolds covers ICE Block
Mechanical Excitation	Mechanical impact, Piston slap, Bearings, Valves, Injection, Fuel pump	Piston connections and Cylinder walls	ICE Block Sump, Timing Cover.

The excitation force, i.e. combustion pressure first distorts the engine structure in an impulsive manner first and then the engine structure begins to vibrate as damped free oscillations, $v(t)$, in major natural modes. This process may be represented as a convolution integral of combustion pressure $p_c(t)$ and impulse response function $h(t)$ of engine structure with acoustic environment included, Equation (3).

$$v(t) = \int_{-\infty}^{\infty} p_c(\tau)h(t-\tau)d\tau \qquad (3)$$

A rise in the cylinder pressure due to combustion pushes the piston from TDC, advancing to BDC. During this movement, the piston impacts with the cylinder walls; this phenomenon, known as piston slap, is another major source of engine noise. Rotating parts, such as the flywheel and front pulley, can excite noise with harmonic components. Mechanical noise consists mainly of piston slap impacts, timing gear rattle, bearing impacts, fuel injection system operation, and valve impacts. Based on the above, the air-borne acoustic signal $S(t)$ could be described by Equation (4):

$$S(t) = s_1(t) + s_2(t) + s_3(t) + n(t) \qquad (4)$$

Where $s_1(t)$ represents harmonic narrow band signal components, i.e. tonal signals at frequencies which are integer multiples of the fundamental rotation speed, $s_2(t)$ is the sum of the

---

[1] A super-Gaussian variable has positive kurtosis: a distribution with a sharp peak and a heavy tails. A sub-Gaussian variable has negative kurtosis: a flat distribution with a light tails.

8

incommensurate narrowband components, i.e., non-harmonically related tonal signals and $s_3(t)$ represents impacts and impulsive signals. $n(t)$ is the broadband random noise and the amplitude of this component depends on many factors such as the type of microphone, location, how far is it from the engine and the room acoustics.

Two complete revolutions of the crank of a diesel engine and consequent airborne acoustic signal are simulated, Equation 4. The simulated airborne acoustic signal sources and the four microphones outputs are illustrated in Figure 7. For simplicity, it is assumed that the transmission of the signal through the engine body is linear, and its disturbance at this stage due to noise is not considered. In order to obtain the virtual observation signals from the sensors, a 4-by-4 random matrix A is selected (Equation 5).

Using the proposed algorithm the source signals are successfully separated, as shown in Figure 8. The first estimated source corresponds to the tonal and harmonic signals, the second is the Gaussian noise, the third is the impacts that occur and the fourth is the transient impulses. An ICA algorithm was also used by the authors to eliminate the disturbance and for noise cancellation from [25].

$$A = \begin{matrix} 0.8750 & -0.3146 & 0.1676 & 0.2332 \\ 0.0765 & -0.9189 & -0.6889 & 0.9085 \\ -0.5153 & -1.5915 & 0.5633 & 2.0624 \\ 0.0776 & -0.2386 & 0.8482 & -0.1762 \end{matrix} \qquad (5)$$
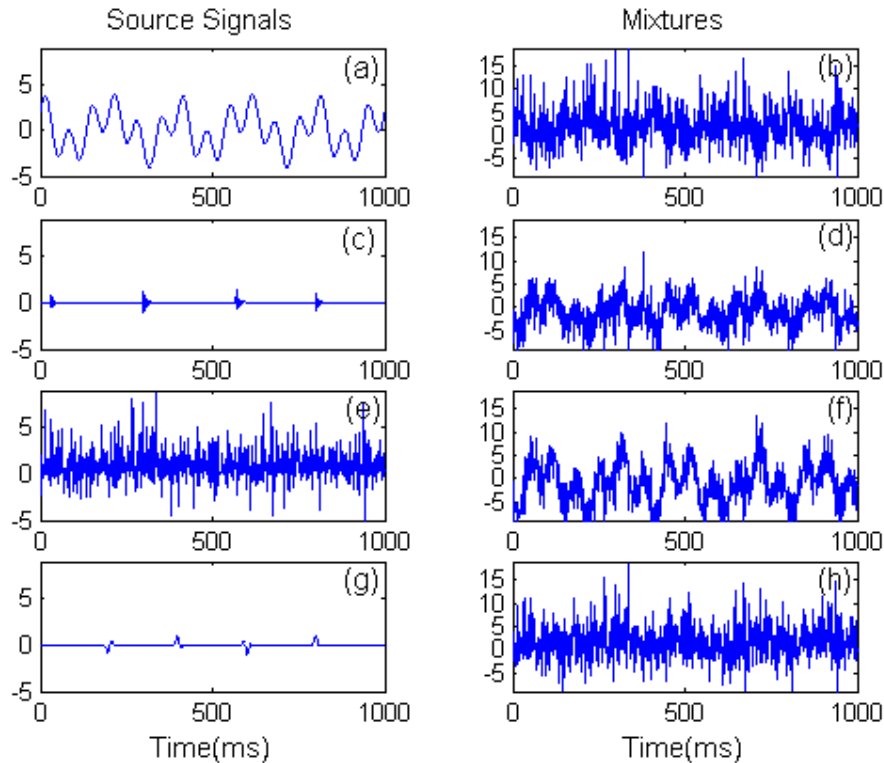

Figure 7 Airborne acoustic signals for two crank revolutions of the engine
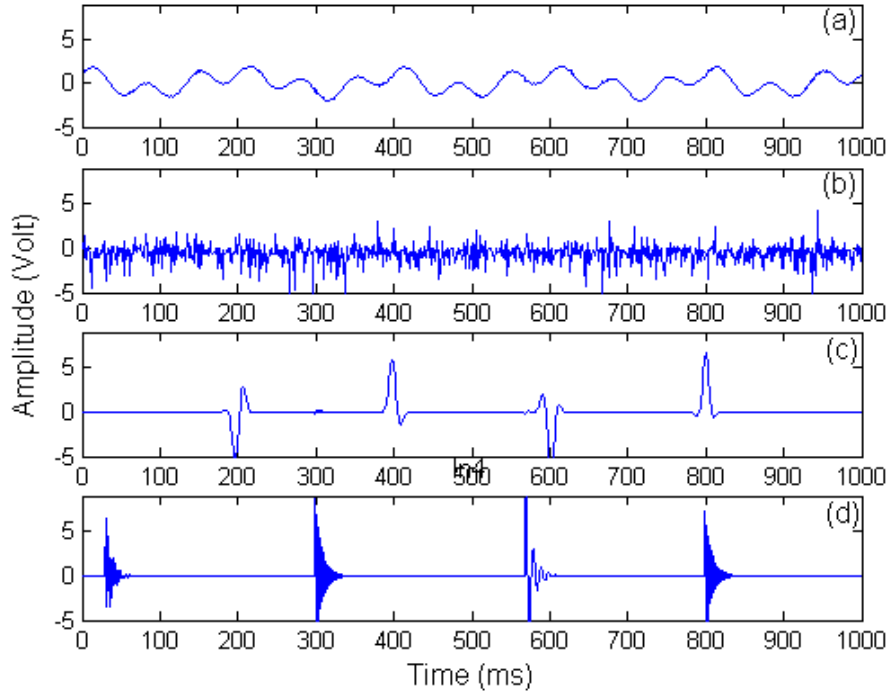
9

Figure 8 Separated airborne acoustic signals

4. EXPERIMENTAL PROCEDURE AND RESULTS

4.1 TEST RIG AND MEASUREMENT STRATEGY

The experiments were performed with a four-stroke, four-cylinder, in-line OHV, direct injection, Ford FSD 425 type diesel engine. The schematic diagram for the test rig and instrumentation are shown in Figures 9.
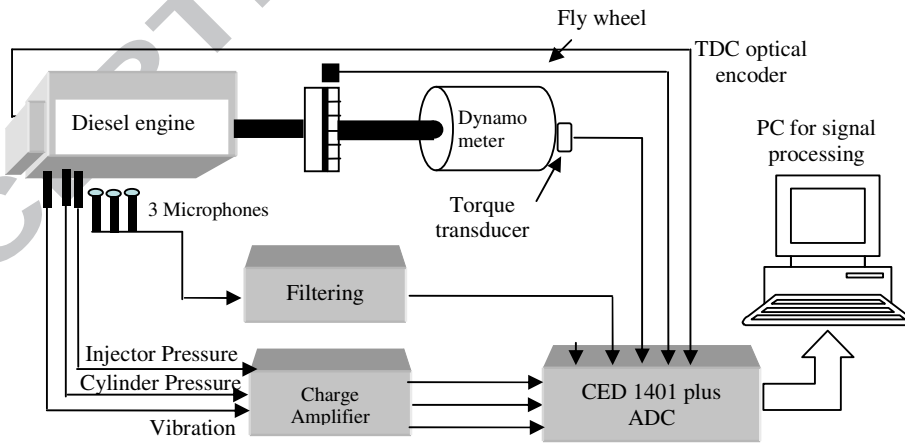

Figure 9 Schematic diagram of engine test system

Three microphones are used to collect air-borne acoustic signals; combustion pressure, injector vibration and injector line pressure are also recorded. The flywheel TDC trigger signal is used to set the start time of data collection so that each data segment is measured at an exact crank position. This is to ensure accurate time domain averaging and rearrangement of data segments. Another trigger

10

signal, from the flywheel gear encoder, is used to measure engine speed from which a certain number of pulses are sent out in each revolution. The data were sampled at 51.7 kHz and 6 data sets consisting of 50 engine cycles were collected in each experiment.
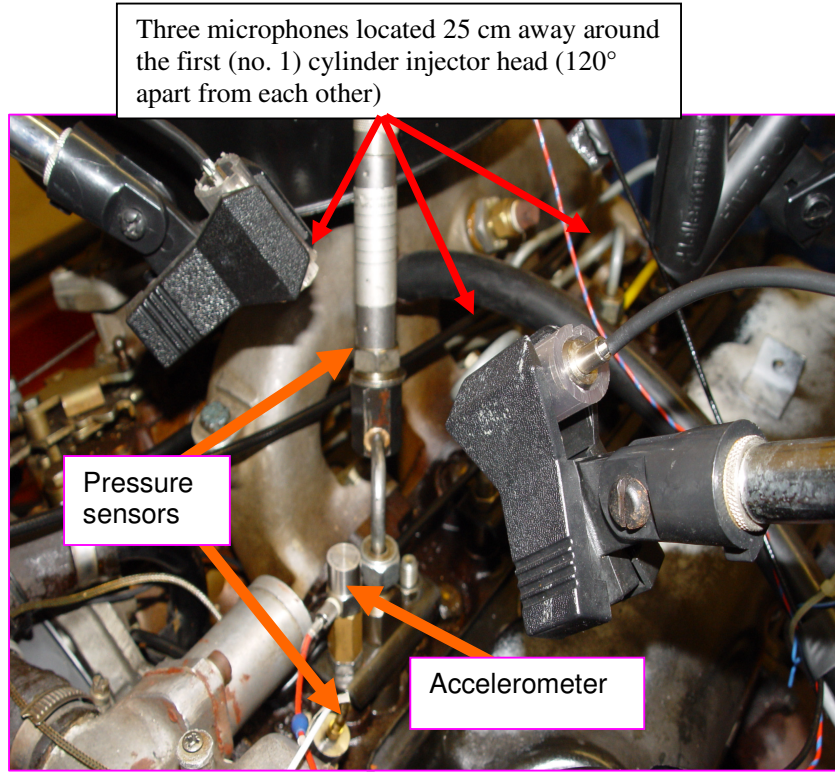

Figure 10 Sensors position around the injector head

As shown in Figure 10, three microphones located 25 cm away around the first (no. 1) cylinder injector head (120° apart from each other) and the experimental data was collected from the diesel engine using a healthy injector running at a speed of 1000 rpm and load of 60 Nm. .

4.2 ICA BASED LGORITHM VALIDATION

Figure 11 overlays the engine air-borne acoustic signal upon the monitored injector body vibration, and cylinder pressure on the fuel injection line pressure. The injector opening and closing angles can easily be located using the injector line pressure or the cylinder pressure, but because of their cost and intrusive nature these methods are not preferred. For the air-borne acoustics it is difficult to see any features, see Figure 1.

The developed condition monitoring method based on the ICA algorithm proposed in section 2 is shown graphically in Figure 12 and may be summarised as follows:

1. Remove the dominant components and the DC components.
2. Pre-whiten input data.
3. Use the learning rule presented in Equation 2 to estimate the demixing matrices for every frequency and calculate separated signals.
4. Transform the separated components into the time-frequency domain using the WVD.
5. Calculate the energy contents of the injection event 11 to 5 degrees before the TDC.
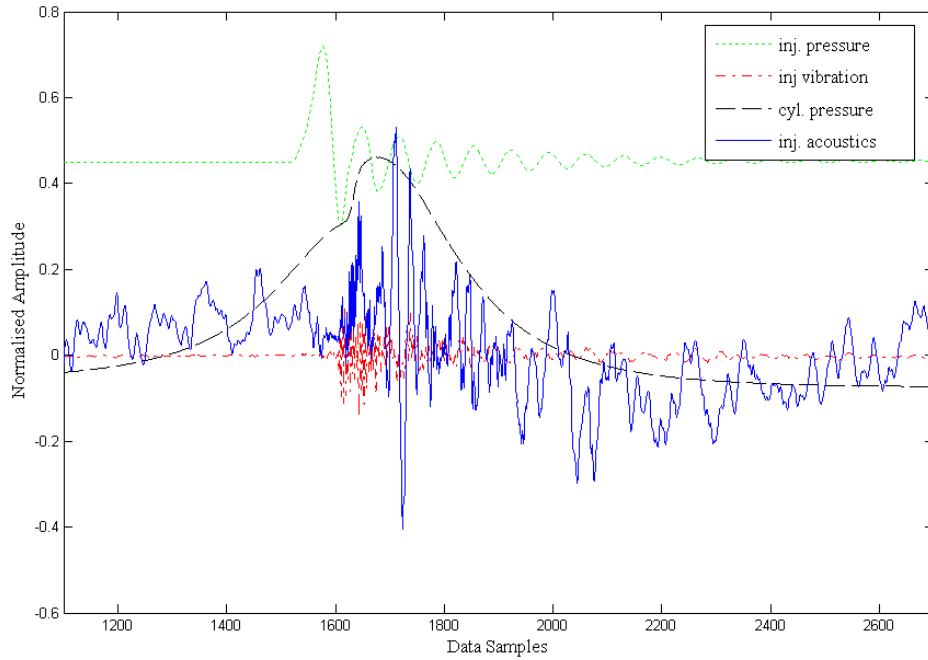
Figure 11 Collected data; normalised injector pressure, injector body vibration, cylinder pressure and engine airborne acoustics.
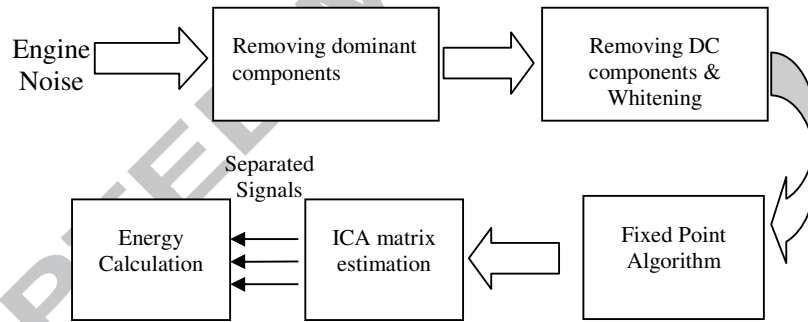

Figure 12 Illustration of the ICA based proposed technique

The beginning time of the injection, which is represented by transient components generated by impacts between the needle and the seat/backstop can be found from the time-frequency domain of one of the recovered ICs -one of the ICA algorithm outputs 7 degrees before top dead centre and at around 15kHz Figure 13(a) -as shown in Figure 13(b). The injector closing event can also be found from the time-frequency domain of the recovered IC shown in Figure 13(e) 5 degrees before top dead centre and at around 9 kHz. The time-frequency representation of IC shown in Figure 13(c) and 13(d) shows the combustion event around the top dead centre (TDC) and the valves open/close at about 9° after the TDC.

One of the most important factors affecting the condition of the injection process is the injector spring stiffness [4, 5]. Any decrease in the stiffness will change the injection time and therefore affect the combustion process and degrade engine performance and increase the emission. The injection pressure was decreased by reducing the injector spring stiffness which decreased the injector opening pressure from 250 to about 230 bars. As a result, earlier injection was expected. Figure 14(d) represents the time-frequency distribution of a faulty injector opening event. It can be seen that the opening impact begins earlier and the amplitudes of the impacts were decreased compared with

12

healthy operation. The closing impact of the faulty injector was recovered in Figure 13(e) and its time-frequency representation is shown in Figure 14(f). More closing impacts at lower intensities could be seen as a result of the weak injector spring. It is also noticed that the combustion event represented in Figure 14(b) is not stable and not good as the combustion process in the healthy case shown in Figure 13(d).

Figure 15 shows normalised energy statistical results, of the proposed monitoring technique, at 60 Nm load and 1000, 1500 and 2000 rpm engine speeds; these energy quantitative results were calculated within a rectangular area around the injection event from 11° BTDC to 5° BTDC.
It can be seen clearly that the energy levels decrease as the injector opening pressure decrease and this becomes clearer at higher speeds.
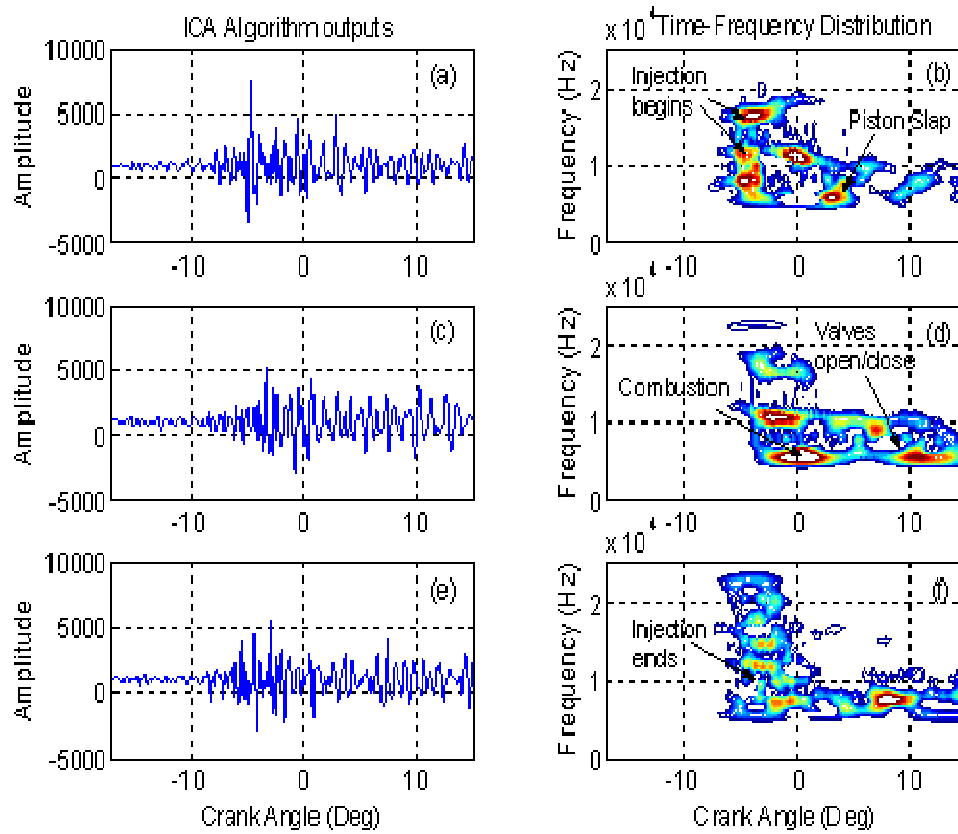

Figure 13 Healthy injector ICA output independent components and their associated WVD
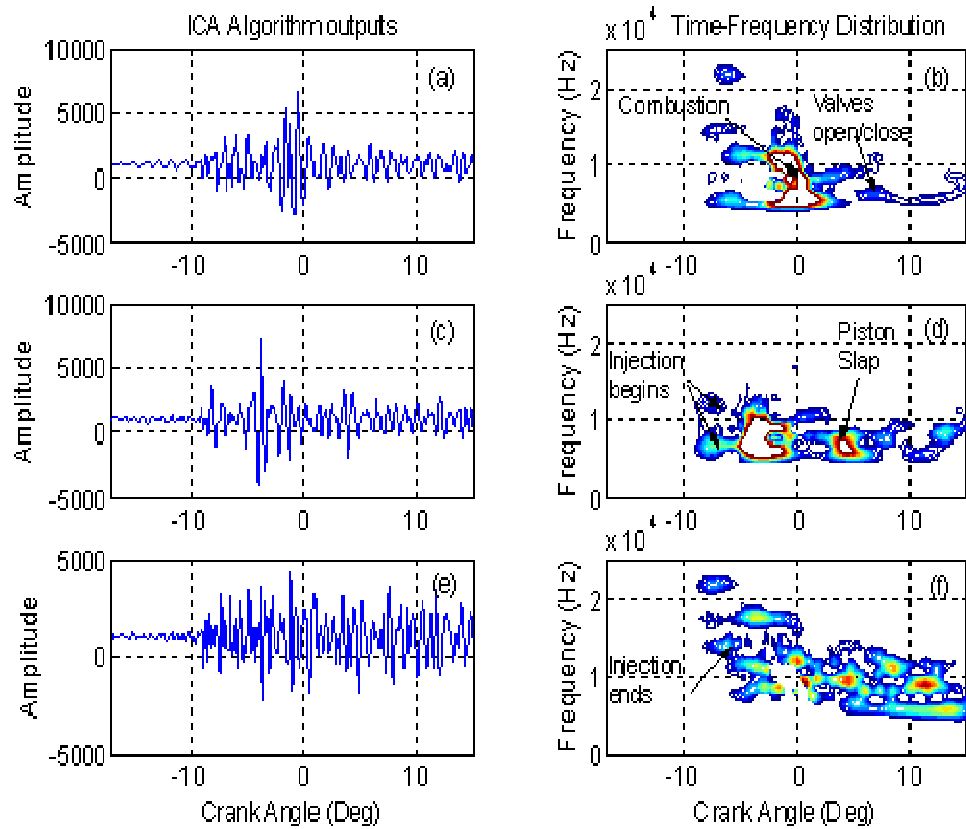
13

Figure 14 Faulty injector ICA output independent components and their associated WVD
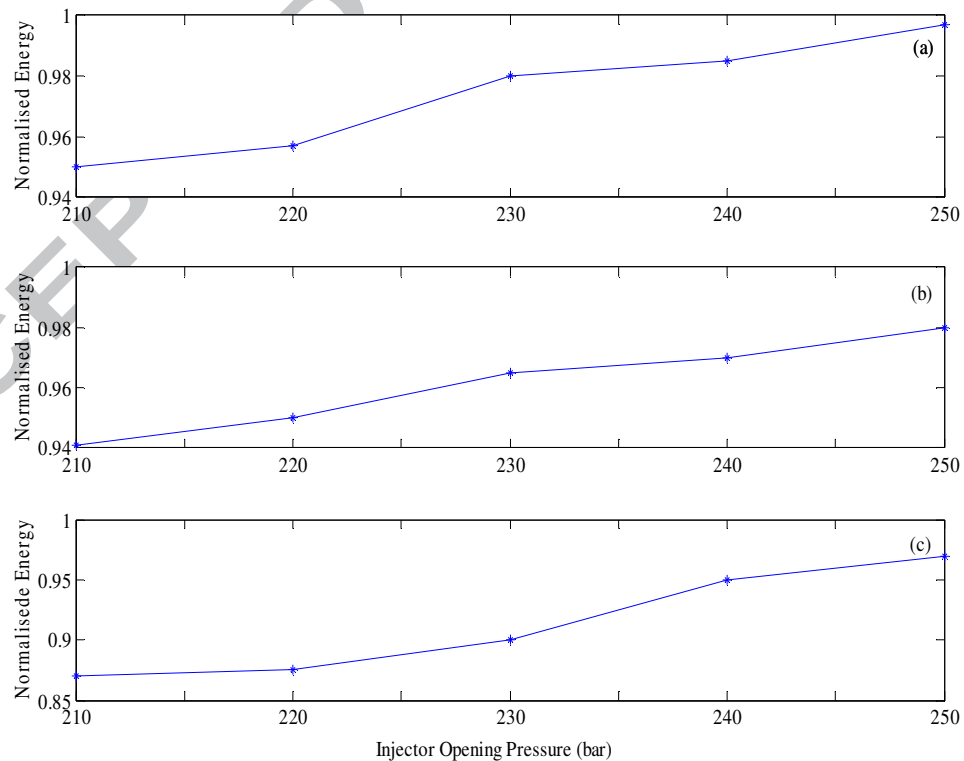

Figure 15 Effect of change in injection pressure, normalised energy comparison at 60 Nm load and speeds of (a) 1000 rpm, (b) 1500 rpm, and (c) 2000 rpm

14

5. CONCLUSIONS

A condition monitoring scheme based on air-borne acoustic signals measurements and independent component analysis has successfully recovered the original sources for simulated diesel engine air-borne acoustic data. The developed scheme separates the real acoustic sources to reduce the affects of the major sources with the stipulation that the sources of the engine air-borne acoustic signal and the transmission channels are unknown. This scheme offers better condition monitoring approaches by enhancing the low energy level events such as the injection process. The optimum microphones locations were found to be 25cm away from the injector head and 120° apart from each other. The developed approach decomposes the air-borne acoustic signals into their sources such as combustion, piston slap, valves motions and fuel injection process. The adopted energy levels calculations and normalised amplitudes offer easier tool to evaluate any abnormality deviation in injection process events and it may be used for other faults associated with this process.

The diesel engine acoustic signals measurements and the signal processing procedures developed in this work show promising results in detecting and diagnosing low energy levels events e.g. injector spring faults. The following few conclusions could be highlighted:

a. Only limited information could be extracted from diesel engine acoustic signals using time domain and frequency domain analysis. The frequency domain analysis gives only information about the frequency components of the measured signals and in the case of diesel engine acoustic condition monitoring these frequency components are dominated by the firing frequencies of the engine and its harmonics.

b. The use of joint time-frequency domain representation; WVD, allows to define dominating combustion frequency. It was found that combustion induced noise is below 5kHz and it is difficult to detect any other acoustic sources such as injection process induced acoustic signals, exhaust and intake valve acoustic sources. Therefore these dominating frequency bands should be carefully filtered.

c. The approaches developed in this article proved to be excellent in detecting small changes in the injector default settings; which make it good condition monitoring tool for such a weak signature. The achieved results are promising and proven to work quiet well at low and high speeds especially under high loads and high speeds; 60 Nm and 2000 rpm.

REFERENCES

1. A. Parlak, H. Yasar, C. Hasimoglu, A. Kolip (2005). The effects of injection timing on NO_x emissions of a low heat rejection indirect diesel injection engine. Applied Thermal Engineering, Volume 25, 3042-3052.

2. T. Priede (1967). Noise of diesel engine injection equipment. Journal of Sound and Vibration, 6(3), 443-459.

3. Q. Hu, S. F. Wu, S. Stottler, R. Raghupathi (2001). Modeling of dynamic responses of an automotive fuel rail system. Part I: Injector. Journal of Sound and Vibration, 245 (5), 801-814.

4. R. S. F. Wu, Q. Hu, S. Stottler, R. Raghupathi (2001). Modeling of dynamic responses of an automotive fuel rail system. Part II: entire system. Journal of Sound and Vibration, 245(5), 815-834.

5. F. Gu, A. D. Ball (1996), Diesel injector dynamics modelling and estimation injection parameters from impact response. Part I: modelling and analysis of injector impacts. Proceedings of Institution of Mechanical Engineers. Part D: Journal of. Automobile Engineering 210(4) 293-302.

6. F. Gu, A. D. Ball, K.K. Rao (1996), Diesel injector dynamics modelling and estimation injection parameters from impact response. Part II: prediction of injection parameters from monitored vibration, Proceedings of Institution of Mechanical Engineers. Part D: Journal of. Automobile Engineering 210(4) 303-312.

15

7. J.D. Gill, R.L. Reuben, J.A. Steel (2000), A study of small HSDI diesel engine fuel injection equipment faults using acoustic emission, in: Proceedings of the EWGAE, 24th European Conference on Acoustic Emission Testing, Paris, France, 281–286.

8. P. Nivesrangsan, J.A. Steel, R.L. Reuben (2007). Acoustic emission mapping of diesel engines for spatially located time series-Part II: Spatial reconstitution. Mechanical Systems and Signal Processing, Volume 21(2), 1084-1102.

9. A. Albarbar (2006), The acoustic condition monitoring of diesel engines, Ph.D. thesis, University of Manchester.

10. A. Albarbar, R Gennish, F. Gu, A. D. Ball (2004), Lubrication oil condition monitoring using vibration and air-borne acoustic measurements. The 7th Biennial ASME Conference on Engineering Systems Design and Analysis, ESDA04, Manchester, July 2004, 58360.

11. A. Albarbar, F. Gu, A. Ball, A. Starr (2007), Internal combustion engine lubricating oil condition monitoring based on vibro-acoustic measurements. Journal of Non Destructive Testing Institution. 49:p.715-719.

12. A. Albarbar, F. Gu, A. Ball, A. Starr (2008), On acoustic measurement based internal combustion engines condition monitoring. Journal of Non-destructive Testing Institution. Insight, 50:p. 30-34.

13. A. Albarbar, S. Alhashmi, R. Gennish, F. Gu, A. D. Ball (2004), Adaptive noise cancelling for enhancing diesel engine air-borne acoustic signal to noise ratio. COMADEM04, Cambridge, pp. 334-343.

14. A. Albarbar, F. Gu, A. D. Ball, A. Starr (2010), Acoustic monitoring of engine fuel injection based on adaptive filtering tecgniques. Applied Acoustics, in press, 10.1016/j.apacoust.2010.07.001.

15. G. Gelle, M. Colas, C. Serviere (2003). Blind Source Separation: A new pre-processing tool for rotating machines monitoring, IEEE Transactions on Instrumentation and Measurement 52(3), 790–795.

16. M. Roam, M. Erling, L. Sibul (2005). A new non-linear adaptive blind source separation approach to gear tooth failure detection and analysis, Mechanical Systems and Signal Processing **16** (5), 719–740.

17. M. Knaak, M. Kunter, D. Filberi (2002). Blind source separation for acoustical machine diagnosis, the 14th International Conference on Digital Signal Processing, Aegean Island of Santorini (Thera), Greece, 159–162.

18. A. Ypma, D. Tax, R. Duin. Robust machine fault detection with independent component analysis and support vector data description, Proceedings of IEEE International Workshop on Neural Networks for Signal Processing, Madison, WI (USA), 23–25 1999, 67–76.

19. X. Tian, J. Lin, K. Fyfe, M. Zuo (2003), Gearbox fault diagnosis using independent component analysis in the frequency domain and wavelet filtering, Proceedings of 2003 IEEE International Conference on Acoustics, Speech, and Signal Processing (ICASSP '03) 2(6–10). 245–248.

20. W. Li. F. Gu, A. Ball, A., Leung, A., Phipps (2001). A Study of the Noise from Diesel Engines Using the Independent Component Analysis. Mechanical Systems and Signal Processing 15(6), 1165-1184.

21. P. Pajunen, A. Hyvärinen, J. Karhunen (1996), Non-linear blind source separation by self-organizing maps, Proceedings of the International Conference on Neural Information Processing, Hong Kong, China, pp. 1207–1210.

22. A. Hyvärinen (1999), Fast and robust fixed-point algorithms for independent component analysis, IEEE Transactions on Neural Networks **10**(3), pp. 626–634.

23. A. Hyvärinen, E. Oja (1997), A fast fixed-point algorithm for independent component analysis, Neural Computation **9**(7), pp. 1483–1492.

24. E. Bingham (2003). Advances in independent component analysis with applications to data mining. PhD thesis, Helsinki University of Technology, Finland.

25. A. Albarbar, M. Regea, M. Elhaj, F. Gu, A. D. Ball (2004), Independent component analysis for enhancing diesel engine air-borne acoustics signal to noise ratio, in: Proceeding of 9th Mechatronics Forum International Conference, Mechatronics04, Ankara, pp 197-207.